

Chapter 2

The counterrotating twin screw extruder

In this thesis, a closely intermeshing counterrotating twin screw extruder is investigated as a polymerisation reactor. A theoretical description of this type of extruder is therefore outlined in this chapter.

A thorough study of the counterrotating twin screw extruder is carried out by Janssen (1978). In this chapter, the main aspects of that study are given and a few corrections are made (e.g. the boundary conditions in section 2.2.6). Furthermore, the theory is validated by residence time distribution measurements. This validation is possible, since the die resistance is determined quantitatively, which is a new aspect in extruder research. This chapter ends by giving the consequences of the experiments for modelling the residence time and residence time distribution of the counterrotating twin screw extruder.

2.1 Twin screw extruders

Twin screw extruders are used in various parts in polymer industry. In most applications, solid polymer pellets are fed to the extruder, which gives three different zones in twin screw extruders. These zones are:

- a solid transport zone, which is filled with polymer pellets from the hopper;
- a melt zone, where the polymer melts;
- a pump zone, which is completely filled with material. In this zone pressure is built up to overcome the die resistance.

In a polymerisation process with a liquid starting material, only two zones can be distinguished in the extruder (figure 2.1):

- a partially filled zone, where the screws are not completely filled with material;
- a pump zone or fully filled zone, where pressure is built up.

The transition from the partially filled zone to the fully filled zone takes place within one pitch length, as will be explained in section 2.2.3.

When the extruder is used as a polymerisation reactor, also a reaction zone can be identified. The position of the reaction zone depends on product properties and on process parameters such as barrel temperature, throughput, screw speed and die resistance. The optimum situation in reactive extrusion is obtained when the reaction takes place in the whole extruder volume. However, in many applications, the extruder used is larger than necessary,

which implies that the extruder is starved fed, resulting in a partially filled zone as illustrated in figure 2.1.

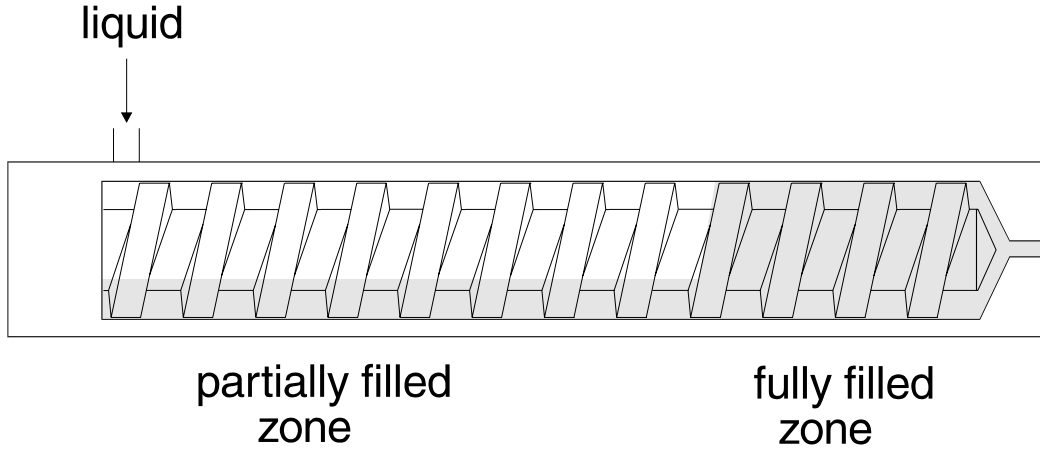


Fig. 2.1 Schematic representation of the two zones in an extruder, which is fed with liquid material

2.2 Extruder theory

The extruder used in this thesis is a counterrotating closely intermeshing twin screw extruder. In this type of extruder, the channel of one screw is blocked by the flight of the other screw (figure 2.2). Therefore, the extruder can be considered as series of separate chambers, which are more or less C-shaped. In the C-shaped chambers, material is transported towards the die by positive displacement. This transport mechanism is characteristic for closely intermeshing extruders. In other types of extruders, material is mainly transported by drag flow. The transport by positive displacement is a stable mechanism, since it is relatively independent of the rheology of the material inside the extruder.

The theoretical throughput Q_{th} is defined as the maximum volumetric displacement rate, which equals the number of C-shaped chambers transported per unit time multiplied by the volume of one chamber:

$$Q_{th} = 2mNV_c \quad (2.1)$$

where N is the screw rotation rate, V_c the volume of a C-shaped chamber and m the number of thread starts. Since the extruder used has a screw with a single thread start, m equals 1. In this chapter, all formulas given are only valid for a single thread start screw ($m=1$). A more extensive description is given by Janssen (1978).

The counterrotating twin screw extruder

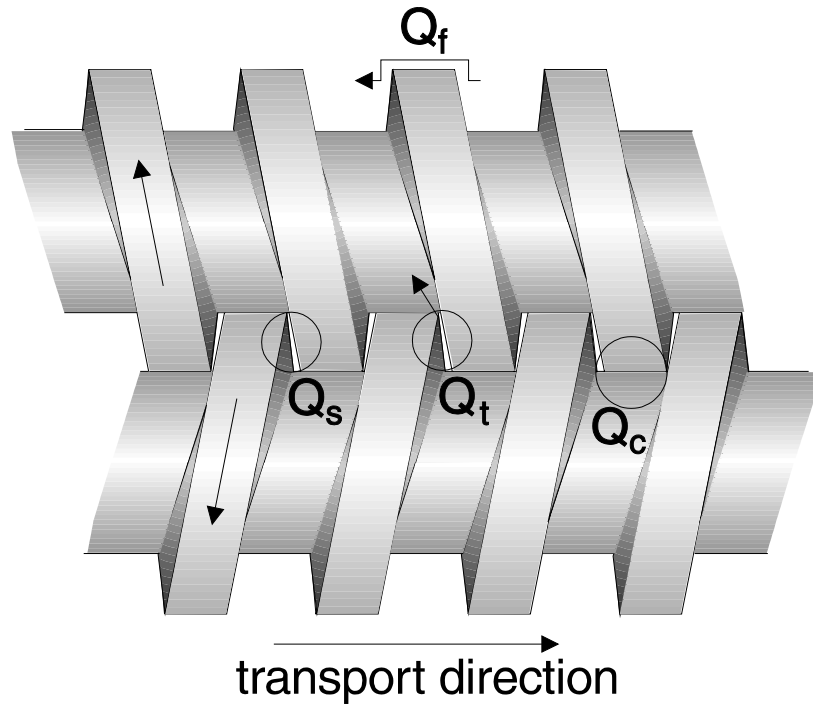


Fig. 2.2 *Closely intermeshing counterrotating screws*

Because of mechanical clearances, the chambers are not completely closed. Leakage flows cause interaction between the chambers. The real volumetric throughput Q is therefore given by:

$$Q = Q_{th} - Q_l \quad (2.2)$$

in which Q_l is the sum of all leakage flows over a cross-section of the extruder. A description of the leakage flows will be given in section 2.2.2.

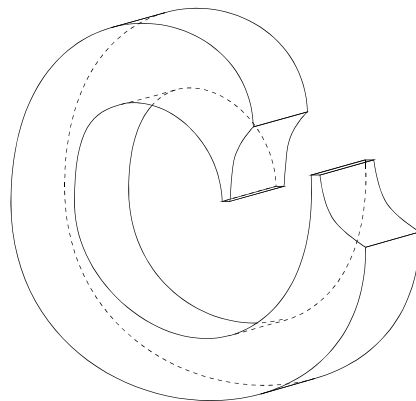


Fig. 2.3 *A C-shaped chamber*

2.2.1 The C-shaped chamber

A closely intermeshing extruder consists of two screws, which rotate in an eight-shaped barrel. Since the screws are closely intermeshing, C-shaped chambers occur. Such a chamber is schematically shown in figure 2.3.

The volume of one C-shaped chamber is very important, since it determines the theoretical throughput (equation 2.1). The volume can be calculated by subtracting the volume of the screws from the barrel house volume. The volume of half the barrel house V_b over one pitch length S is given by:

$$V_b = \left\{ \left(\pi - \frac{\alpha_s}{2} \right) (R + \delta)^2 + \left[(R + \delta) - \left(\frac{H - \sigma}{2} \right) \right] \sqrt{R(H - \sigma) - \left(\frac{H - \sigma}{2} \right)^2} \right\} S \quad (2.3)$$

with:

$$\alpha_s = \arccos \left(\frac{2R - H + \sigma}{2R} \right)$$

The relevant parameters are shown in figure 2.4 and figure 2.5.

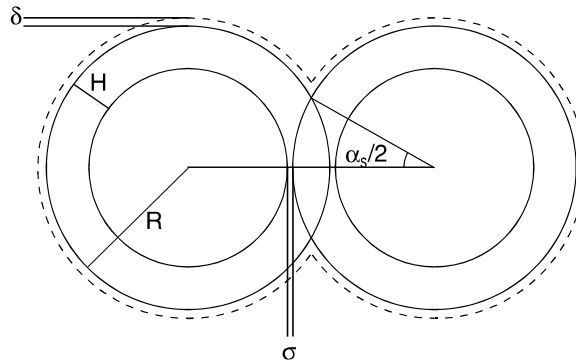


Fig. 2.4 Cross-section of the barrel house

Obviously, the screw volume is determined by the volume of the of the screw root and the screw flights. The volume of the screw root V_r over one pitch length S is given by:

$$V_r = \pi(R - H)^2 S \quad (2.4)$$

The counterrotating twin screw extruder

The volume of the screw flight V_f equals:

$$V_f = 2\pi \left[\left(RH - \frac{H^2}{4} \right) B_{fl} + \left(RH^2 - \frac{2}{3} H^3 \right) \tan \psi \right] \quad (2.5)$$

The total volume of one chamber V_c can be calculated by subtracting the volume of the screw from the volume of the barrel house. For a single tread start screw, the volume equals:

$$V_c = V_b - V_r - V_f \quad (2.6)$$

The volume of one C-shaped chamber of the extruder used in this thesis is 7.31 ml.

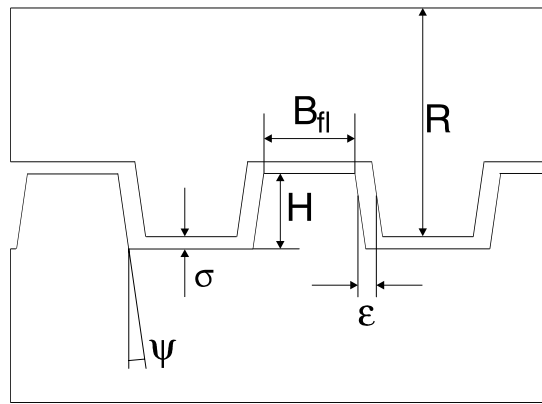


Fig. 2.5 Cross-section of the screws

2.2.2 The leakage flows

Equation 2.2 shows that the throughput of the extruder equals the theoretical throughput minus the leakage flows. In the counterrotating twin screw extruder, four leakage flows occur as a result of four gaps that be distinguished (figure 2.2):

- the flight gap, which is a clearance between the barrel and the flight of the screws;
- the tetrahedron gap, which originates from a gap between the flight walls. This gap resembles a tetrahedron and it is the only gap that connects chambers on the opposite screws;
- the calander gap, which is formed by the clearance between the flight of one screw and the bottom of the channel of the other screw. This gap resembles a calander;
- the side gap, which is a clearance between the flight walls of the screws, perpendicular to the plane through the screw axes.

The leakage flows are driven by interchamber pressure differences ΔP_c and by the conveying of the moving surfaces. The leakage flows driven by conveying of the moving surfaces can be interpreted as the amount of material that is not scraped from the walls.

Chapter 2

In general form, the leakage flows are given by:

$$Q_l = AN + B \frac{\Delta P_c}{\eta} \quad (2.7)$$

where A and B are geometrical constants, and η the viscosity of the material inside the extruder. The values of the geometrical constants for the extruder used are listed in table 2.1. These values are calculated by using the dimensions of the screw as given in table 2.6 (see appendix at the end of this chapter). As can be seen in table 2.1, the leakage flow through the tetrahedron gap is only pressure driven. There is no drag flow in this gap, because the walls move in opposite direction. If an interchamber pressure difference exists, the leakage flow through the tetrahedron gap is the most important in the extruder used. Roughly 65% of the total pressure driven leakage flow passes this gap. When no interchamber pressure difference exists, the leakage flow through the calander gap is most important. Since the flight gap width is very small, the flow through this gap is almost negligible.

Table 2.1 *Geometric constants. A_c means the geometrical constant A belonging to the calander gap, etc.*

Symbol	place of the gap	value
A_c	calander gap	$1.559 \cdot 10^{-6} \text{ m}^3$
A_s	side gap	$5.782 \cdot 10^{-7} \text{ m}^3$
A_f	flight gap	$6.270 \cdot 10^{-8} \text{ m}^3$
A_t	tetrahedron gap	0
B_c	calander gap	$2.663 \cdot 10^{-10} \text{ m}^3$
B_s	side gap	$4.791 \cdot 10^{-11} \text{ m}^3$
B_f	flight gap	$2.152 \cdot 10^{-13} \text{ m}^3$
B_t	tetrahedron gap	$1.158 \cdot 10^{-9} \text{ m}^3$
A		$4.399 \cdot 10^{-6} \text{ m}^3$
B		$1.787 \cdot 10^{-9} \text{ m}^3$

The total leakage flow can be calculated by solving a mass balance over the cross-section of the extruder. Since the leakage flows go from one chamber to different other chambers, the leakage flow can be calculated via:

$$Q_l = Q_t + 2Q_f + 2Q_s + 2Q_c \quad (2.8)$$

As stated before, the C-shaped chambers can be schematically represented by separate chambers, which are transported towards the die. The chambers are connected by the leakage flows as illustrated in figure 2.6.

The counterrotating twin screw extruder

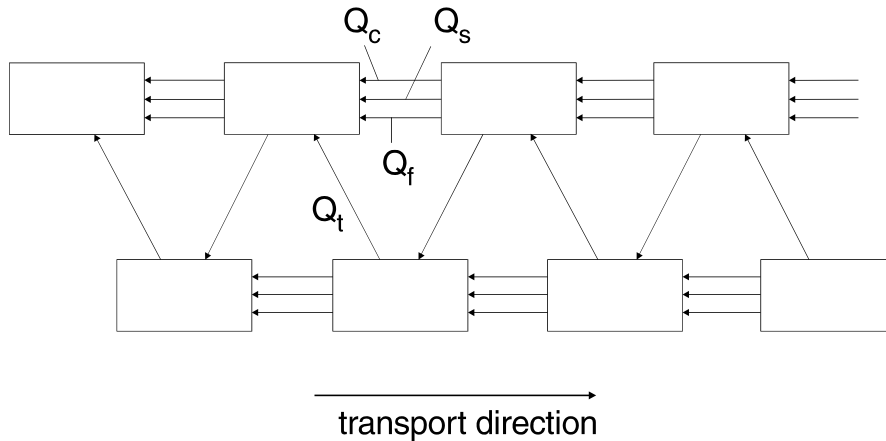


Fig. 2.6 *Schematic representation of the interaction between the C-shaped chambers by the leakage flows for a single thread screw*

2.2.3 The partially filled zone

When an extruder is fed with a liquid (or a polymer melt), two zones can be distinguished: a fully filled zone and a partially filled zone. A closer look at figure 2.7 reveals that the partially filled zone can be divided into three zones.

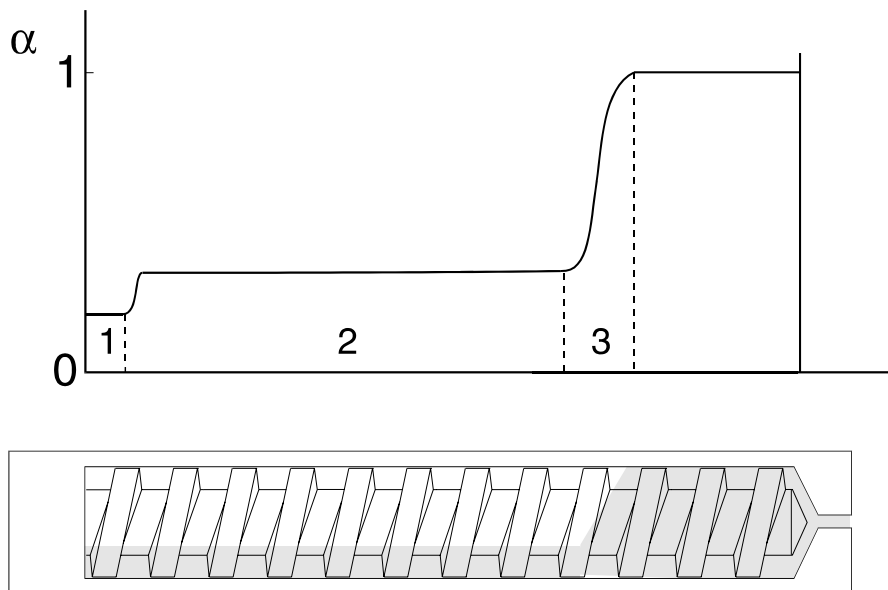


Fig. 2.7 *The degree of fill versus the length of the extruder*

Zone 1 is the feed zone. Due to the fact, that no leakage flows occur in the first chamber (the flow can not go back), the degree of fill α can be calculated by using:

Chapter 2

$$\alpha = \alpha_r = \frac{Q}{Q_{th}} \quad (2.9)$$

In zone 2, the degree of fill is somewhat higher than the relative throughput α_r , since some leakage flow is likely to occur. The degree of fill therefore equals:

$$\alpha = \frac{Q + Q_{l,pfz}}{Q_{th}} \quad (2.10)$$

The amount of leakage flow in the partially filled zone $Q_{l,pfz}$ is studied experimentally in section 2.3.5. In order to describe $Q_{l,pfz}$ adequately, the function $f(\alpha)$ is introduced. This function indicates the fraction of drag induced leakage flow that should be taken into account in the partially filled zone. The value of the function $f(\alpha)$ lies between 0 and 1, and is considered to be dependent on the degree of fill α . Since no interchamber pressure difference exists in the partially filled zone, the leakage flow in the partially filled zone is given by:

$$Q_{l,pfz} = f(\alpha)AN \quad (2.11)$$

In the literature, several assumptions are made for $f(\alpha)$. Speur (1988) and Janssen (1979) assumed $f(\alpha) = 0$, when a solid feed is used. For most solid feeds, this assumption is valid, although Jager (1992) and Chen (1993) found that for respectively maize grits and polystyrene some leakage flow occurs in the partially filled feed zone. For a liquid feed, some leakage flow will always occur, as a result of which the degree of fill is underestimated by using $f(\alpha) = 0$.

Pieters (1993) obtained good results in predicting the residence time by assuming $f(\alpha) = 1$, which means that the total non-pressure driven leakage flows are taken into account in the partially filled zone. The throughput was always smaller than $0.2 \cdot Q_{th}$ in that study. In another study (De Graaf 1996), the leakage flow was assumed to be linearly dependent on the degree of fill. In formula form:

$$f(\alpha) = \alpha$$

The third zone is the transition to the fully filled zone. Within one pitch, the pressure induced leakage flows, which come from the last chamber of the fully filled zone, fill the chambers completely. The short transition zone was experimentally observed by Janssen (1978).

2.2.4 The fully filled zone

The counterrotating twin screw extruder

The fully filled zone is the pump zone of the extruder. In this zone, pressure is built up, which is needed to overcome the die resistance. The length of the fully filled zone L can be calculated by means of the number of fully filled chambers v_f . For an isoviscous liquid, the pressure built up per chamber is constant, which implies:

$$v_f = \frac{P_{die}}{\Delta P_c} \quad (2.12)$$

The die pressure P_{die} is determined by the die resistance (K^{-1}), throughput Q and viscosity η of the material in the die:

$$P_{die} = \frac{Q\eta}{K} \quad (2.13)$$

By combining equations 2.2, 2.7, 2.12 and 2.13, the number of fully filled chambers can be expressed as a function of geometrical constants, screw speed and throughput.

$$v_f = \frac{BQ}{K(Q_{th} - Q - AN)} \quad (2.14)$$

Equation 2.14 shows that for an isoviscous liquid, the number of fully filled chambers is independent of the viscosity of the material inside the extruder. From equation 2.14, the fully filled length can be calculated by using:

$$L = v_f S \quad (2.15)$$

2.2.5 The mean residence time

Generally, twin screw extruder are partially filled. The volume V that is filled with liquid is given by:

$$V = v_f V_c + (v_{tot} - v_f) \alpha V_c \quad (2.16)$$

where v_{tot} is the total number of chambers in the extruder.

When a die with a volume V_{die} is attached to the extruder, the mean residence time τ for the combination of extruder and die is given by:

$$\tau = \frac{v_f V_c + (v_{tot} - v_f) \alpha V_c + V_{die}}{Q} \quad (2.17)$$

2.2.6 Flow profiles in the chambers

Chapter 2

The flow pattern in a C-shaped chamber is very important for a good understanding of the working of an extruder. The flow in a C-shaped chamber is mainly three-dimensional (Speur 1988). For reasons of simplicity, we will only discuss some two-dimensional flow patterns as described in literature.

The geometry of a C-shaped chamber is very complicated. Therefore, the chamber will be simplified to a rectangle (figure 2.8). This representation implies that the depth of the chamber is small compared to the radius and that the pitch of the screw is not very large. Furthermore, the movement of the flights at the beginning and at the end of the chamber is neglected.

The transport of material is caused by the movement of the C-shaped chamber towards the die due to the rotation of the screw. Within the chamber, the surface of the screw drags the material in a tangential direction towards the end of the chamber (this means in the direction of the feed zone), which results in pressure differences inside the chamber. The net resulting flow of drag and pressure equals the leakage flow from one chamber to other chambers. The amount of leakage flow, and therefore the throughput, determines whether the pressure flow is opposite to or in the same direction as the drag flow.

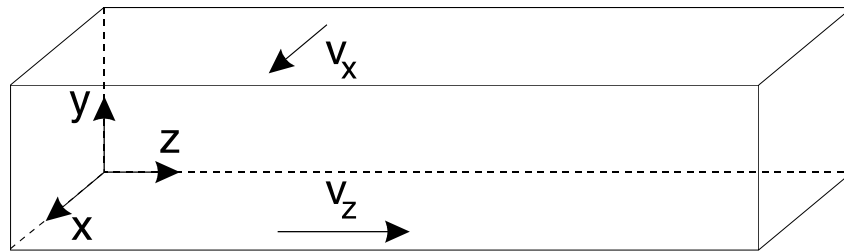


Fig. 2.8 Rectangular representation of a chamber

An approximation of the flow profile in the chamber can be obtained by making some further assumptions. First of all, the depth of the chamber is small compared to the width, the liquid is incompressible and shows Newtonian behaviour. Furthermore, the inertia forces are neglected. The momentum equation for the flow in the tangential direction towards the end of the chamber reduces to:

$$\frac{1}{\eta} \frac{dP_t}{dz} = \frac{d^2 v_z}{dy^2} \quad (2.18)$$

with the boundary conditions:

$$v_z(0) = \pi N D \cos \phi + N S \sin \phi = \frac{\pi N D}{\cos \phi} \quad (2.19)$$

$$v_z(H) = N S \sin \phi$$

where ϕ is the screw angle (figure 2.9). A positive velocity v_z means that the velocity is in the down-chamber direction. If the depth of the chamber H is not negligible compared to the diameter D of the screw, it is better to use $(D-2H)$ instead of D in equation 2.19.

The counterrotating twin screw extruder

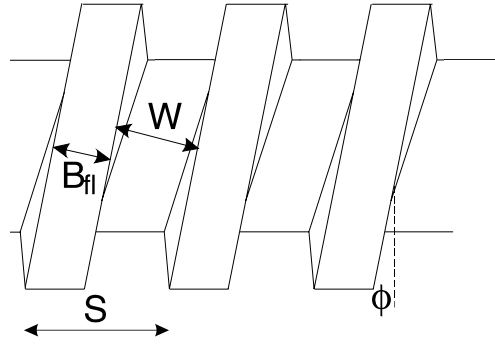


Fig. 2.9 Dimensions of a screw

The solution of equation 2.18 is:

$$v_z(y) = \frac{1}{2\eta} \frac{dP_t}{dz} y(y-H) - \frac{v_z(0) - v_z(H)}{H} y + v_z(0) \quad (2.20)$$

From equation 2.20, the throughput in the down-chamber direction can be derived. It equals:

$$Q_z = \frac{\{v_z(H) + v_z(0)\}WH}{2} - \frac{WH^3}{12\eta} \frac{dP_t}{dz} \quad (2.21)$$

The pressure difference $\frac{dP_t}{dz}$ can be expressed as function of the relative throughput by using equation 2.21:

$$\frac{dP_t}{dz} = \frac{6\eta}{WH^3} [\{v_z(H) + v_z(0)\}WH - 2(1 - \alpha_r)NV_c] \quad (2.22)$$

By combining equation 2.20 and 2.22, the velocity in the z-direction versus the height can be derived:

$$v_z(y) = 3 \left\{ \frac{v_z(H) + v_z(0)}{H^2} - \frac{2(1 - \alpha_r)NV_c}{WH^3} \right\} y(y-H) - \frac{v_z(0) - v_z(H)}{H} y + v_z(0) \quad (2.23)$$

Figure 2.10 shows the velocity profiles in the chamber for several values of the relative throughput. The number at the curves gives the value for relative throughput α_r . In the reactive extrusion experiments described in this thesis, α_r is always smaller than 0.1.

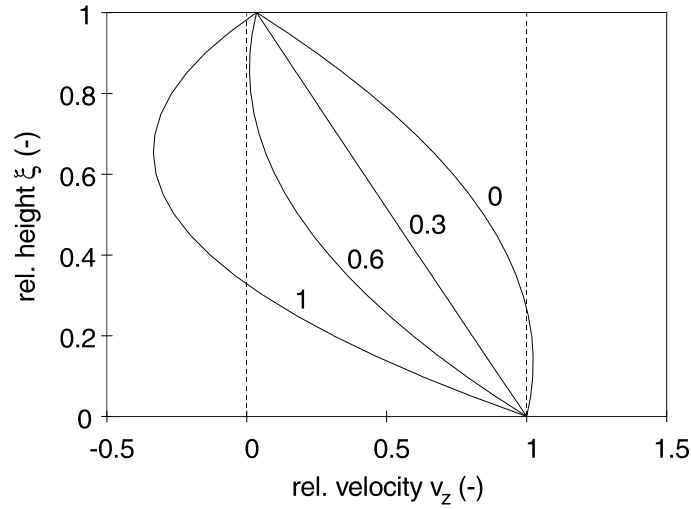


Fig. 2.10 The relative velocity $\frac{v_z(\xi)}{v_z(H)}$ versus the relative height $\xi = \frac{y}{H}$. The numbers next to the curves refer to the various α_r for which the velocity profile is calculated

In a similar way, the velocity profile in the cross-chamber direction can be calculated. For a shallow chamber, the momentum equation can be written as:

$$\frac{1}{\eta} \frac{dP_x}{dx} = \frac{d^2 v_x}{dy^2} \quad (2.24)$$

with the boundary conditions:

$$\begin{aligned} v_x(0) &= 0 \\ v_x(H) &= NS \cos \phi \end{aligned} \quad (2.25)$$

When it is assumed that the leakage flow through the flight gap is negligible, which means that the net flow is zero, the velocity profile is given by:

$$v_x(y) = \frac{y(3y - 2H)}{H^2} v_x(H) \quad (2.26)$$

This profile only depends on the height in the chamber (figure 2.11).

The counterrotating twin screw extruder

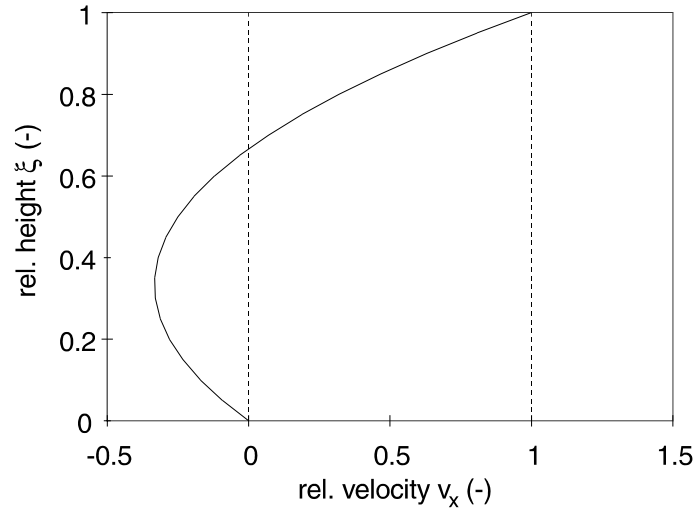


Fig. 2.11 The relative velocity $\frac{v_x(\xi)}{v_x(H)}$ versus the relative height $\xi = \frac{y}{H}$

2.2.7 Pressure differences inside the chamber

Due to the rotation of the screw, pressure differences arise both in the axial and in the tangential direction of the chamber. This pressure gradient in tangential direction may be positive or negative, depending on the amount of leakage flows through the chamber. The pressure gradient, which is given by equation 2.22, equals the pressure difference over one chamber divided by the length of the chamber. To calculate the pressure difference inside the chamber, the length of the chamber has to be determined. This length is given by:

$$L = \frac{(2\pi - \alpha_s)R}{\cos \phi} \quad (2.27)$$

By combining equations 2.22 and 2.27, the pressure difference inside one single chamber equals:

$$\Delta P_t = \frac{6(2\pi - \alpha_s)R\eta}{WH^3 \cos \phi} [2(1 - \alpha_r)NV_c - \{v_z(H) + v_z(0)\}WH] \quad (2.28)$$

The pressure difference ΔP_t in equation 2.28 is negative when the pressure gradient is positive in down-chamber direction. This situation is obtained at high relative values of the throughput. At a low throughput, the pressure gradient is positive in the channel direction. This means that the flows in the chamber due to drag flow and pressure flow are in the same

direction, namely in the down-chamber direction. Figure 2.12 shows the effect of the throughput on the pressure gradient schematically.

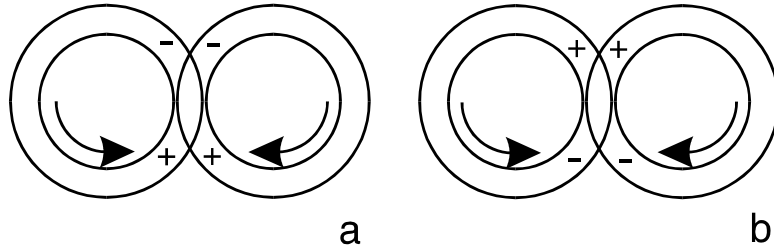


Fig. 2.12 The pressure gradient inside the chambers in the case of a high (a) and a low throughput (b)

The importance of the down-chamber pressure difference is plotted in figure 2.13, in which the pressure ratio is defined as:

$$\Pi = \frac{\Delta P_t}{2\Delta P_c + \Delta P_t} \quad (2.29)$$

The interchamber pressure difference is multiplied by 2, because of the definition of ΔP_c (see nomenclature). Figure 2.13 also shows that at low values of the throughput, the tangential pressure gradient is in the same direction as the interchamber pressure difference, while at high values of the throughput this gradient is in the opposite direction. No interchamber pressure difference exists for a relative throughput α_r of 0.32.

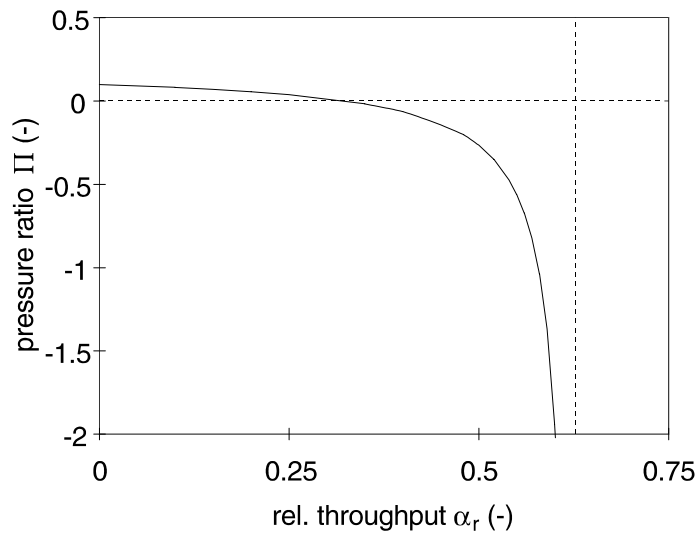


Fig. 2.13 The pressure ratio Π versus the relative throughput

The existence of the tangential pressure difference implies that at a low throughput, the number of fully filled chambers, as calculated by equation 2.14, is (slightly) underestimated. At a high throughput, the number of fully filled chambers can be far more than the number of chambers as predicted by equation 2.14. The maximum throughput of the extruder is obtained when:

$$2\Delta P_c = -\Delta P_t \quad (2.30)$$

which implies that the pressure built up by the extruder is zero. For the extruder used, this situation is obtained for a relative throughput α_r of 0.63.

2.3 Residence time and residence time distribution

In this section, residence time distribution (RTD) measurements are performed in order to determine the mean residence time in the extruder quantitatively. This mean residence time is used for calculating the average degree of fill.

A method to obtain the RTD is to inject a tracer pulse into the system and measure the output tracer concentration as a function of time (Danckwerts 1953). For ease of comparison, the output concentration curves are usually normalised. The function that describes the RTD is the exit age function $E(t)$, which is defined as:

$$E(t) = \frac{C(t)}{\int_0^{\infty} C(t)dt} \quad (2.31)$$

The mean residence time τ is given by:

$$\tau = \int_0^{\infty} t E(t)dt \quad (2.32)$$

The spread in residence time is characterised by the standard deviation σ_t or the variance σ_t^2 :

$$\sigma_t^2 = \int_0^{\infty} (t - \tau)^2 E(t)dt \quad (2.33)$$

The reduced standard deviation σ_θ can be obtained by:

$$\sigma_\theta = \sqrt{\frac{\sigma_t^2}{\tau^2}} \quad (2.34)$$

2.3.1 Experimental

The extruder used for the RTD-experiments was a Rollepaal extruder. It is a counterrotating twin screw extruder, which is extensively described in section 4.2. The screw geometry and some other extruder data are listed in table 2.6 (see appendix at the end of this chapter). To the extruder, one of the dies listed in table 2.2 is attached. The dies used in this chapter are linear tubes, which means that their resistances can be calculated by using the Hagen-Poiseuille-equation, in which L_{die} and R_{die} are respectively the length and the inner radius of the tube:

$$K^{-1} = \frac{8L_{die}}{\pi R_{die}^4}$$

Table 2.2 *The dies used for RTD measurements. A higher die number means a larger die resistance*

die	reciprocal die resistance K (10^{-11} m^3)	die volume (10^{-6} m^3)
I	61.9	37.3
II	4.60	31.5
III	1.52	31.1

In the other chapters, a die with a variable resistance is used. For this die, the resistance was determined experimentally.

2.3.2 Materials

The residence time distribution was studied by using glycerine at room temperature. Glycerine is a Newtonian fluid, with a viscosity of 0.9 Pa s. The tracer used was a solution of 2.62 mmol/l Congo Red (from Merck) in glycerine. When the extrusion process had reached steady state, 5 ml of the tracer solution was injected in the extruder at the feed end. Every 10 to 15 seconds, samples were taken at the die end in disposable cuvettes (Griener Labortechnik Kuvetten Makro), until a few minutes after all colour had disappeared in the extrudate. The absorption of the samples was measured at a wavelength of 511.5 nm using a Philips PU 8730 UV/VIS scanning spectrophotometer.

2.3.3 The RTD-measurements

The residence time distribution in extruders has been studied quite often. For the distribution, many models have been introduced. An overview is given by Bounie (1988). However, most studies estimate the hold-up experimentally, because the die resistance is not determined in those studies. This section describes the hold-up, and evaluates the usefulness of equation 2.14 in predicting the number of fully filled chambers. Moreover, the RTD-measurements are used for estimating the function $f(\alpha)$ in equation 2.11. Furthermore, the

influences of the throughput, screw speed, die resistance and relative throughput are investigated.

Glycerine is not very viscous when compared to polymer melts. However, since it behaves as a Newtonian liquid, glycerine is very suitable for theoretical considerations. Dimensionless numbers indicate whether or not the results are representative for highly viscous liquids. First of all, the Reynolds number determines the flow regime. For extruders, the number is defined as:

$$Re = \frac{\text{inertia forces}}{\text{viscous forces}} = \frac{\rho ND^2}{\eta} \quad (2.35)$$

In the experiments described in this section, the Re-number lies between 0.4 and 1.9, which means that the flow is laminar, and in most cases there is creeping flow, just as by materials with a high viscosity.

The second dimensionless number is the Dean-number that gives the ratio of centrifugal forces and viscous forces

$$De = \frac{\text{centrifugal forces}}{\text{viscous forces}} = Re \sqrt{\frac{H}{D}} \quad (2.36)$$

Its value lies between 0.14 and 0.70 in all experiments. This means that centrifugal forces can be neglected in these experiments.

The Jeffrey's number describes the influence of the gravity forces on the experiment. For extruders, it is defined as (Todd 1975):

$$Je = \frac{\text{gravity forces}}{\text{viscous forces}} = \frac{D\rho g}{\eta N} \quad (2.37)$$

For all experiments, the value for Jeffrey lies between 660 to 3300. The meaning of the value is discussed in section 2.3.5.

2.3.4 Results: the influence of throughput and screw rotation rate

The results of the RTD-measurements are described in this section. The influence of throughput and screw speed are measured and compared to theory.

When the throughput is increased, the die pressure increases. This results in a longer fully filled zone. The increase in fully filled length is even more enhanced by the fact that the interchamber pressure difference decreases at increasing throughput. Apart from the length of the fully filled zone, the degree of fill in the partially filled zone will increase. This means that the average hold-up in the extruder will increase. Figure 2.14 shows the influence of the throughput on the mean residence time. Since the residence time decreases less than the throughput increases, it can be concluded that the average hold-up is increased. Therefore,

Chapter 2

our results correspond well to the theory and are contrary to the results obtained by Rauwendaal (1981), who found a constant hold-up for various values of the throughput. The reason for the constant hold-up, as measured by Rauwendaal, is not clear yet.

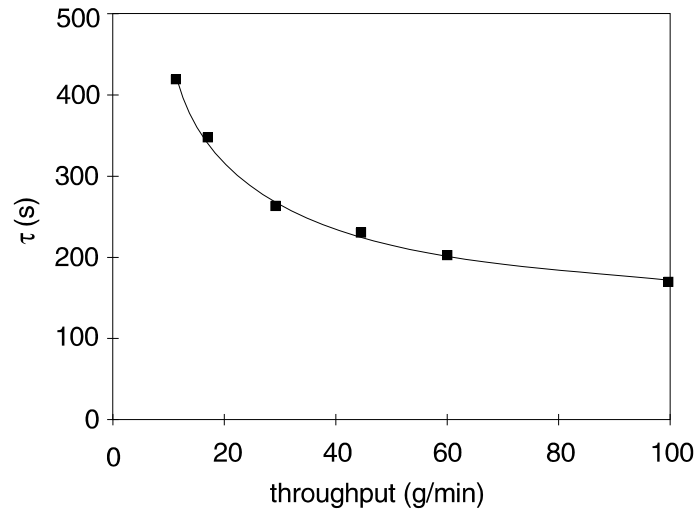


Fig. 2.14 *The influence of the throughput on the mean residence time (die II)*

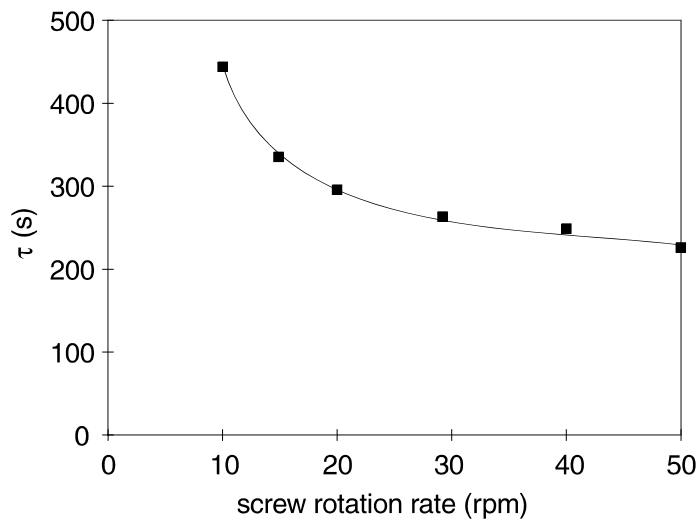


Fig. 2.15 *The influence of the screw rotation rate on the mean residence time (die II)*

Figure 2.15 shows the effect of the screw rotation rate on the residence time. A higher screw speed reduces the number of fully filled chambers and the degree of fill. These two effects account for the decrease in residence time.

Figure 2.16 shows the effect of the throughput on the mean residence time, while the relative throughput (i.e. throughput divided by screw speed) remains constant. A higher throughput results in a decrease in residence time, but the mean residence time is not inversely proportional with the throughput. This result was not expected, because both the degree of

The counterrotating twin screw extruder

fill and the number of fully filled chambers should remain constant when the relative throughput is kept constant. Since calculations show that the number of fully filled chambers is more or less constant, it can be concluded that the degree of fill increases with increasing throughput and screw speed. It is probable that this increase in hold-up is due to the relatively low viscosity of glycerine. This effect will be explained in section 2.3.5, in which theory and experiments concerning the average hold-up in the extruder will be compared, after having studied the partially filled zone in the next section.

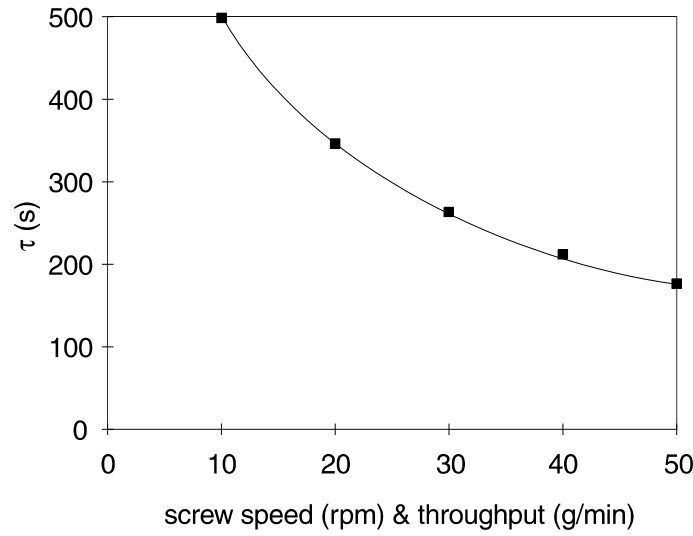


Fig. 2.16 The influence of the throughput at constant relative throughput. A value of 20 on the x-axis means a throughput of 20 g/min at a screw speed of 20 rpm etc.

2.3.5 The partially filled zone

To determine the degree of fill in the partially filled zone, die I was applied. The resistance of this die was chosen in such a way that according to equation 2.14 less than 1 chamber was fully filled. The results of the experiments are shown in table 2.3.

Table 2.3 The degree of fill in the partially filled zone

Q (g/min)	N (rpm)	τ (s)	v_f (-)	α_r (-)	α (-)
29	30	213	0.2	0.07	0.25
30	50	176	0.1	0.04	0.24
49	50	144	0.2	0.07	0.29
62	30	135	0.6	0.14	0.33
98	30	114	1.0	0.23	0.45

Table 2.3 shows that the degree of fill α in the partially filled zone is significantly larger than the relative throughput α_r . This implies that a certain amount of leakage flow occurs in the partially filled zone.

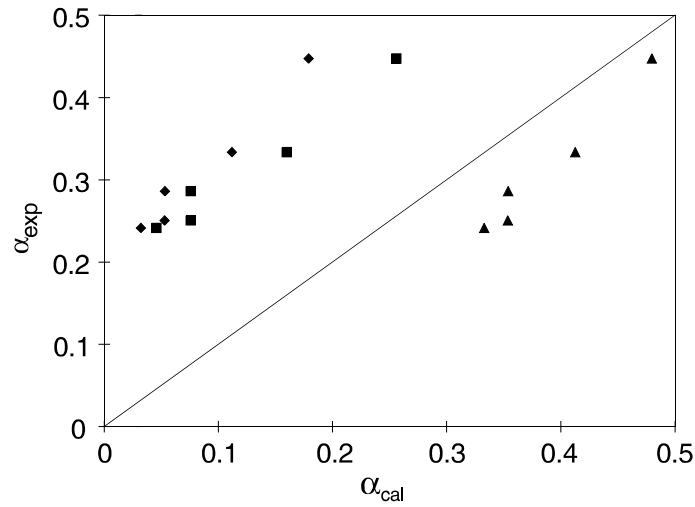


Fig. 2.17 The calculated degree of fill versus the experimental value for $f(\alpha) = 0$ (\diamond), $f(\alpha) = 1$ (\blacktriangle) and $f(\alpha) = \alpha$ (\blacksquare)

As already described in section 2.2.3, several predictions are made for the degree of fill in the partially filled zone by assuming a certain function $f(\alpha)$. Figure 2.17 shows the results of these theories. None of the theories predicts the degree of fill correctly, but it can be seen that for a good prediction of the degree of fill, one should choose a value for $f(\alpha)$ between α and 1. A value of 0.7 predicts the degree of fill for these experiments quite well (figure 2.18). However, for the throughput of 98 g/min, the degree of fill is even higher, which indicates that almost all non-pressure driven leakage flows should be taken into account.

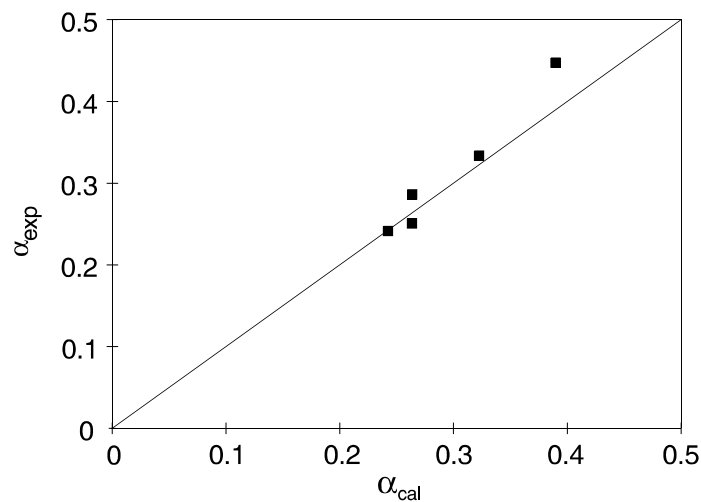


Fig. 2.18 The calculated degree of fill versus the experimental value for $f(\alpha) = 0.7$

The counterrotating twin screw extruder

As already stated in section 2.3.4, the low viscosity of glycerine results in an underestimation of the degree of fill. This can be explained by the fact that at low screw speed, gravity force plays an important role in the extrusion process. Leakage flow occurs mainly in the calander gap in the partially filled zone (table 2.1). In the extruder used, this gap is 2 cm above the bottom side of the barrelhouse. As a result of this, two competing effects influence the amount of leakage flow. The gravity force holds material onto the bottom of the barrel house, while viscous forces lift the material towards the calander gap. This means that the gravity force results in a decrease in amount of leakage flow, since it prevents material to enter the calander gap. When the screw speed is increased, the influence of the gravity diminishes (as indicated by a lower Je -number) which results in a larger leakage flow.

The effect of the screw speed on the average degree of fill is indicated in figure 2.19. As expected, the degree of fill increases when the screw speed is increased. Furthermore, it can be seen that the increase in hold-up levels off at higher screw speed, suggesting an asymptotic value for the degree of fill. Curve fits show that the value of the asymptote lies between 34 and 40. The horizontal line in the figure indicates the value for the hold-up when $f(\alpha) = 1$, which means that all non pressure driven leakage flows are taken into account. This line therefore refers to the highest possible value for the hold-up. It seems that this value is indeed the asymptotic value for the experiments. This implies that when gravity forces can be neglected, the total leakage flow AN should be taken into account in the partially filled zone. If the extrapolation is correct, the influence of the gravity is negligible at a screw speed of 200 rpm or higher. This means that the gravity force can be neglected when:

$$Je < 150 \tag{2.38}$$

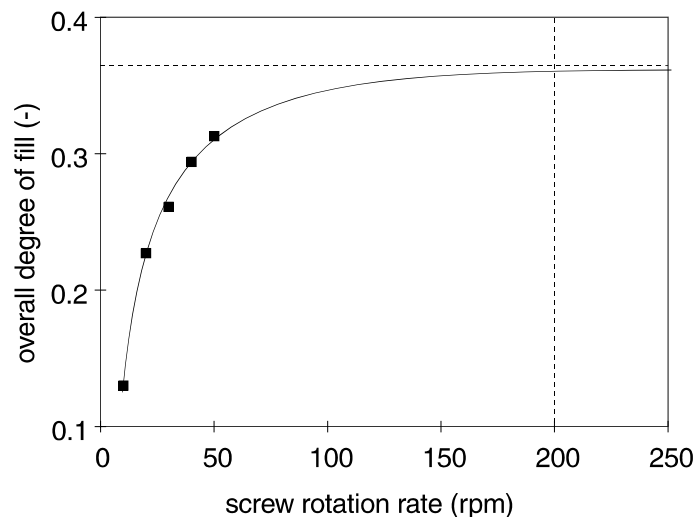


Fig. 2.19 *The effect of the screw speed on the overall hold-up at constant relative throughput, die I, die II with 4 fully filled chambers.*

The experiments described in this section show that the amount of leakage flow that occurs in the partially filled zone is quite large. By trial and error it was found that a good prediction of the degree of fill can be obtained by using $f(\alpha) = 0.7$. However, industrial extruders have a higher throughput and more viscous materials (this means a lower Je -number). In those situations, the total leakage flow AN should be taken into account for a good prediction of the degree of fill in the partially filled zone.

2.3.6 The number of fully filled chambers

The number of fully filled chambers can be predicted theoretically by using equation 2.14. By applying dies with different resistances, the number of fully filled chambers can be determined experimentally. Figure 2.20 shows the principle of the measurements. According to equation 2.14, the number of fully filled chambers is less than 1 when die I is used. When die II or III is applied, a certain number of chamber is completely filled. The number of fully filled chambers can be calculated by comparing the mean residence time obtained by die I and the mean residence time of the experiments with die II or III. The degree of fill in the partially filled zone is determined in section 2.3.5, and is assumed to be independent of the number of fully filled chambers.

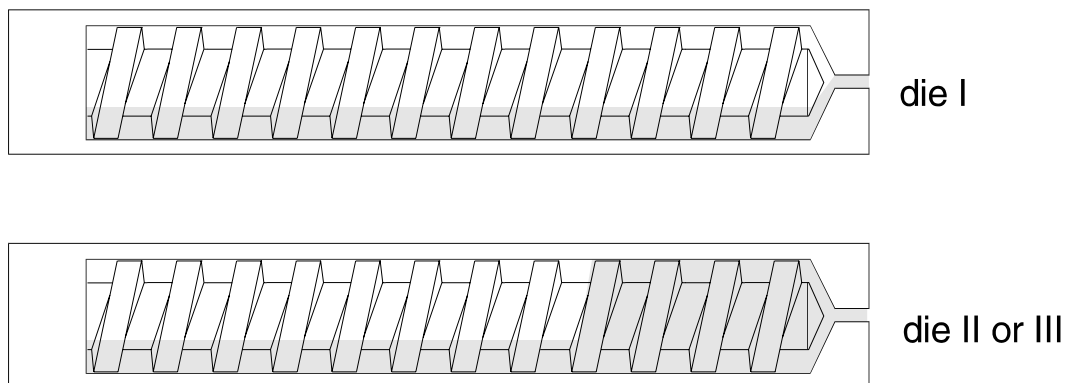


Fig. 2.20 An extruder with and without fully filled chambers

Figure 2.21 shows the results of the experiments. The number of fully filled chambers, which is predicted by equation 2.14 is less than the number of chambers determined experimentally. When the calculated number of chambers is increased with 30%, the experimental and calculated values correspond rather well (figure 2.22).

The reason for the effect as shown in figure 2.21 is not completely clear yet. The discrepancy between theory and experiment gets even worse by taking into account the pressure difference (ΔP_t) inside the chamber. As illustrated in figure 2.13, the pressure gradient is in the same direction as the interchamber pressure difference at a low throughput, which means that the number of fully filled chambers is overestimated by equation 2.14. Also the viscosity of glycerine does not seem to cause the differences between the calculated and experimental values.

The counterrotating twin screw extruder

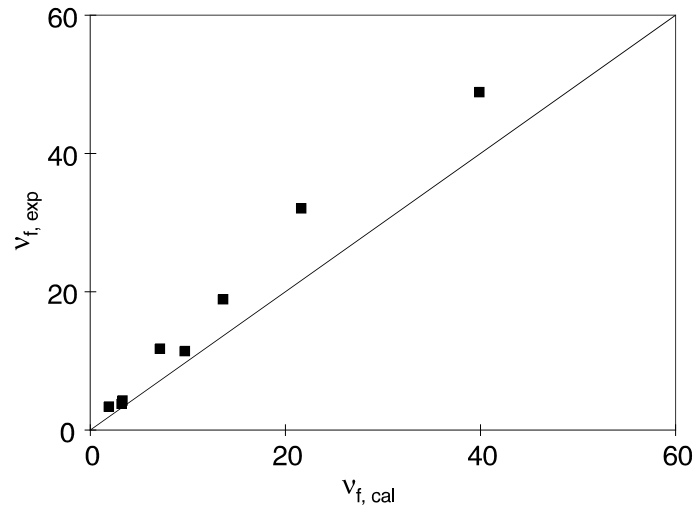


Fig. 2.21 Parity plot of the number of fully filled chambers

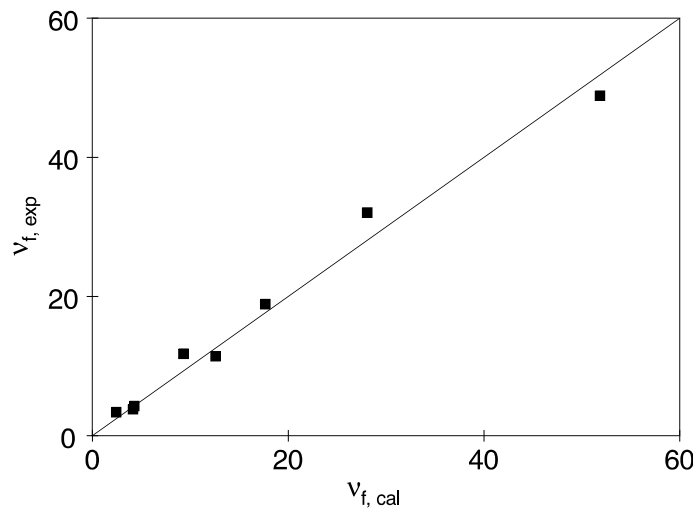


Fig. 2.22 As figure 2.21, but the calculated number of chambers is increased with 30%

2.3.7 Reproducibility and sensitivity analysis

In order to decide whether the differences between the number of fully filled chambers, which are calculated and which are experimentally determined are significant or not, additional study was performed.

For the reliability of the RTD-measurements, two tests were performed. First of all, some experiments were performed twice (table 2.5, exp.: 5&6, 10&11, 21&22). The difference in mean residence time in experiments 5&6 and 21&22 was negligible, while in experiments 10&11 a difference of less than 4% was obtained. In other words, the reproducibility seems sufficient. The second test was to check if all the tracer that was added to the extruder could be detected in the output of the extruder. The results of this test are shown in the last column of table 2.5 (see appendix at the end of this chapter). In the experiments tested, the total

Chapter 2

amount of tracer found in the outlet of the extruder was almost identical to the amount of tracer injected in the feed zone. The two tests indicate that the RTD-measurements are quite reliable.

Another aspect, which can be important for the prediction of the fully filled length, is the geometry of the screw. Wear, for example, can influence the geometrical constants. Therefore, the major screw parameters were changed theoretically in order to determine their influence on the number of fully filled chambers and chamber volumes. The results are shown in table 2.4. This table demonstrates that the influence of the value of the screw parameters is very large, especially on the pump capacity of the extruder. For counterrotating, closely intermeshing twin screw extruders as used in this study, the influence of wear is very pronounced. However, we think that the effect described in table 2.4 is not sufficient for explaining the discrepancies in the number of fully filled chambers, since the measurement of the dimensions of the screws was very accurate.

Table 2.4 *Influence of several screw parameters on the number of fully filled chambers and chamber volume*

R (cm)	V_c (ml)	v_f (-)	S (cm)	V_c (ml)	v_f (-)
1.950	8.52	27.7	2.30	6.84	4.7
1.980	7.72	10.9	2.38	7.31	7.2
1.990	7.44	8.2	2.40	7.42	7.9
1.995	7.31	7.2	2.45	7.72	9.9
2.000	7.17	6.3	2.50	8.01	12.2

2.4 Evaluation of the existing extruder models

The distribution in residence time of the counterrotating twin screw extruder has been studied several times. In principle, two ways of modelling the RTD exist. One method is to describe the overall RTD (Bounie 1988, Jager 1992, Potente 1989); another method is to describe the RTD of one chamber, after which the RTD of the extruder is calculated (Janssen 1979, Chen 1993, Chen 1995).

Jager (1992) presented a reactor model, which could be used for corotating, as well as counterrotating twin screw extruders. An interesting aspect of that model was, that not all the liquid that passed a leakage gap flows through the entire chamber, as in most other extruder models (e.g. figure 2.6). Potente (1989) presented a distribution function that predicts the residence time distribution of a specific counterrotating twin screw extruder. The distribution function, which consisted of a four parameter fit, turned out to be only dependent on the minimum residence time and the mean residence time. Unfortunately, Potente did not generalise the results. However, the studies by Jager, Bounie and Potente show that the residence time distribution of a counterrotating extruder can be readily fit by several reactor models.

More interesting are the predictive models as described by Janssen (1979) and Chen (1993, 1995). These models assume a residence time distribution function for the C-shaped chambers, after which the residence time distribution function of the extruder is calculated. Janssen (1979) assumed the chamber to be ideal mixed and obtained a very good agreement in the case of melting polypropene in a extruder with double thread starts screws. However, Speur (1988) showed that at lower values of the throughput ($\alpha_r < 0.25$), the model of ideally mixing shows severe discrepancies with the experiments. Since in reactive extrusion the throughput is always relatively low, the model by Janssen is not very useful for describing the extruder as a polymerisation reactor. Such a model, as described by Ganzeveld (1993), showed therefore major discrepancies between model simulations and experimental results.

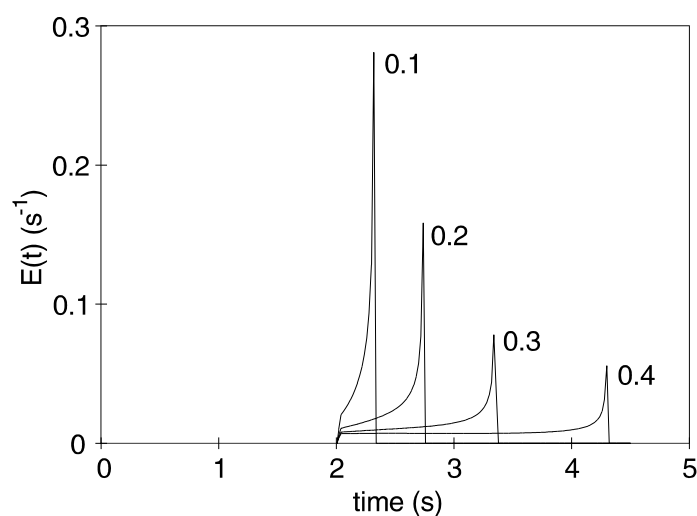


Fig. 2.23 *The distribution in residence times of material that leaves a C-shaped chamber. The number at the curves gives the value for α_r .*

Chen (1993, 1995) used the theory of Pinto and Tadmor (1970), which was developed for single screw extruders, to describe the distribution in residence time in a C-shaped chamber. If the theory of Pinto (1970) is applied to one chamber, a residence time distribution as shown in figure 2.23 is obtained. When this model is compared to the model of Janssen (1979), this model of Chen has the advantage that it takes a certain breakthrough time into account, which will be present in practice. The model of Chen showed a small variance in residence time distribution for a C-shaped chamber, but this variance increases with the throughput (figure 2.23). With this theory, Chen obtained excellent results for an intermeshing (Chen 1993) as well as a non-intermeshing (Chen 1995) counterrotating twin screw extruder. These excellent results are remarkable since the authors made mistakes in developing the residence time distribution function (equation 11 and 12, Chen 1993) for the C-shaped chamber. Therefore, we were not able to reproduce their results. Besides, the theory of Pinto (1970) is a rather crude approximation for the flow profile in the chamber, because the height of the chamber is not negligible in comparison to the width, which is a very important assumption in the theory of Pinto. This assumption will be valid for most

Chapter 2

single screw extruders, but not for closely intermeshing twin screw extruders, which mostly possess deep channels. Besides, in a chamber of twin screw extruders, the pressure flow is in the same direction as the drag flow for lower values of the throughput, while in single screw extruders, these flows are in the opposite direction. Pinto (1970) did not validate his theory for drag and pressure flows in the same directions, which makes the theory not very reliable for this situation. Therefore, studies that use the theory of Pinto for twin screw extruders (e.g. Speur 1988) should be interpreted with some suspicion.

However, the method to predict a RTD of the extruder by using the RTD of one C-shaped chamber seems promising. The RTD of one C-shaped chamber can be calculated by using three-dimensional flow simulations, as shown by Li (1993). For a non-intermeshing counterrotating twin screw extruder, the flow pattern was simulated by Fukuoka (1994) and Chu (1994a). Chu (1994a) used the three-dimensional flow simulation for calculating a RTD of the extruder. In another study, Chu (1994b) showed the possibilities of using the same method for simulating the extruder as a polymerisation reactor. Although the method seems promising, Chu did not compare the values obtained by simulation to experimental results.

Another aspect in modelling the RTD of a counterrotating twin screw extruder is the question whether a leakage flow passes a chamber completely or not. Especially the flow through the tetrahedron gap can pass a chamber without flowing through it (Janssen 1978). Therefore, the model as shown in figure 2.6 has probably to be extended, similar to the model of Jager (1992).

2.5 Conclusions

Although the counterrotating twin screw extruder has been studied quite often, a predictive model for the residence time distribution for this type of extruder is not available yet. A model for the RTD first of all needs a prediction of the mean residence time. This mean residence time can be calculated by determining the degree of fill in the partially filled zone and the number of fully filled chambers. To calculate the number of chambers, the die resistance should be determined quantitatively.

In order to validate the theory, residence time measurements were performed by using glycerine. The experiments showed that the number of fully filled chambers were slightly underestimated by the traditional theory (about 30%), while a good prediction of the degree of fill in the partially filled zone was obtained by taking 70% of non-pressure driven leakage flows into account. For industrial extrusion processes, the total non-pressure driven leakage flows should be taken into account.

For the description of the RTD of an extruder, the theory outlined by Chen (1993) seems very promising. However, for a good estimation of the RTD of the C-shaped chamber, 3D flow simulations in combination with particle tracking should be used.

Table 2.5 *Experimental results*

Exp. no.	die	Q (g/min)	N (rpm)	τ (s)	$\sigma(\theta)$ (-)	% tracer
1	II	9.3	10	498	0.52	
2	II	11.3	30	420	0.48	
3	II	17.0	30	348	0.53	
4	II	20.0	20	346	0.45	
5	II	29.9	10	444	0.24	
6	II	29.9	10	443	0.33	
7	II	29.2	15	335	0.45	
8	II	30.0	20	296	0.47	
9	I	29.3	30	213	0.47	98
10	II	29.2	30	263	0.43	98
11	II	29.3	30	273	0.40	
12	III	29.6	30	370	0.38	98
13	II	29.7	40	249	0.51	
14	I	29.5	50	176	0.56	101
15	II	29.7	50	226	0.50	
16	II	39.8	40	212	0.41	
17	II	44.6	30	231	0.35	
18	I	48.9	50	144	0.51	96
19	II	50.4	50	176	0.49	
20	I	61.7	30	135	0.49	
21	II	60.0	30	200	0.34	97
22	II	60.9	30	203	0.34	
23	III	60.0	30	326	0.46	108
24	I	98.0	30	114	0.40	
25	II	99.7	30	169	0.37	
26	III	98	30	263	0.12	98

Nomenclature

A	geometrical constant for the non pressure driven leakage flows	m^3
A_c	geometrical constant for the calander gap	m^3
A_f	geometrical constant for the flight gap	m^3
A_s	geometrical constant for the side gap	m^3
A_t	geometrical constant for the tetrahedron gap	m^3
b_s	barrel width	m
B	geometrical constant for the pressure driven leakage flows	m^3
B_c	geometrical constant for the calander gap	m^3
B_f	geometrical constant for the flight gap	m^3

Chapter 2

B_f	width of the screw flight	m
B_s	geometrical constant for the side gap	m^3
B_t	geometrical constant for the tetrahedron gap	m^3
$C(t)$	concentration	mol/l
D	diameter of the screw	m^3
De	Dean-number	-
$E(t)$	exit age function	s^{-1}
$f(\alpha)$	function that indicates the fraction of non-pressure driven leakage flows	-
g	gravity force constant	m/s^2
h_c	centre line	m
H	height of the screw flight	m
Je	Jeffrey number	-
K	reciprocal die resistance	m^3
L	length of (a part of) the screw	m
L_{dir}	length of the die	m
m	number of thread starts	-
N	screw rotation rate	s^{-1}
P	pressure	Pa
P_c	pressure inside the chamber, see also ΔP_c	Pa
P_{die}	die pressure	Pa
P_t	see ΔP_t	Pa
P_x	see ΔP_x	Pa
Q	throughput	m^3/s
Q_c	leakage flow through the calander gap	m^3/s
Q_f	leakage flow through the flight gap	m^3/s
Q_l	total leakage flow	m^3/s
$Q_{l, p/z}$	leakage flow in the partially filled zone	m^3/s
Q_s	leakage flow through the side gap	m^3/s
Q_t	leakage flow through the tetrahedron gap	m^3/s
Q_{th}	theoretical throughput	m^3/s
Q_z	throughput through the chamber	m^3/s
R	radius of the screw	m
R_{dir}	inner radius of the die	m
Re	Reynolds number	-
S	pitch of the screw	m
t	time	s
v_x	velocity in x -direction	m/s
v_y	velocity in y -direction	m/s
v_z	velocity in z -direction	m/s
V	volume	m^3
V_b	volume of (half) the barrel house	m^3
V_c	volume of a C-shaped chamber	m^3
V_{die}	volume of the die	m^3

The counterrotating twin screw extruder

V_r	volume of the root of the screw	m^3
V_f	volume of the screw flight	m^3
X	constant	
$x, y,$		
z	coordinates	-
α	degree of fill	-
α_r	relative throughput	-
α_s	overlap angle of the screws	rad
δ	flight gap width	m
ΔP_c	pressure difference of two adjacent chambers (this means chambers on opposite screws. The pressure difference of two chambers on the same screw is $2\Delta P_c$)	Pa
ΔP_t	tangential pressure difference inside a chamber	Pa
ΔP_x	pressure difference in cross-chamber direction	Pa
ε	side gap width	m
ϕ	pitch angle	rad
η	viscosity	Pa s
Π	pressure ratio	-
ρ	density	kg/m^3
σ	calander gap width	m
σ_t	standard deviation	s
σ_θ	reduced standard deviation	
τ	mean residence time	s
V_f	number of fully filled chambers	-
V_{tot}	total number of chambers after injection point	-
ψ	flight angle	rad

References

- Bounie D., J. of Food Eng., vol. 7., p. 223-46 (1988)
- Chen L., Hu G.H., Lindt J.T., Pol. Eng. Sci., vol. 35, no. 7, p. 598-603 (1995)
- Chen L., Pan Z., Hu G.H, AIChE Journal, vol. 39, no. 9, p. 1455-64 (1993)
- Chu L., Min K., Pol. Eng. Sci., vol. 34, no. 12, p. 986-94 (1994a)
- Chu L., Min K., Pol. Eng. Sci., vol. 34, no. 12, p. 995-1004 (1994b)
- Danckwerts P.V., Chem. Eng. Sci., vol. 2, no. 1, p. 1-13 (1953)
- Fukuoka T., Min K., Pol. Eng. Sci., vol. 34, no. 13, p. 1033-46 (1994)
- Ganzeveld K.J., Capel J.E., Van der Wal D.J., Janssen L.P.B.M., Chem. Eng. Sci., vol. 49, no. 10, p. 1639-49 (1994)
- Graaf R.A. de, PhD-thesis, University of Groningen, The Netherlands (1996)
- Jager T., PhD thesis, PhD-theses, Agricultural University Wageningen, The Netherlands (1992)

Chapter 2

- Janssen L.P.B.M, Hollander R , Spoor M.W., Smith., AIChE Journal, vol. 25, no. 2, p. 345-51 (1979)
- Janssen L.P.B.M., Twin Screw Extrusion, Elseviers Sci. Publ. Comp., Amsterdam (1978)
- Li T., Manas-Zloczower I., AIChE symposium series, no. 293, vol. 89, p. 31-36 (1993)
- Pieters R.T., PhD-thesis, University of Groningen, The Netherlands, (1993)
- Pinto G., Tadmor Z., Pol. Eng. Sci. vol. 10, no. 5, p. 279-88 (1970)
- Potente H., Schultheis S.M., Intern. Pol. Proc., vol. IV, no. 4, p. 255-61 (1989)
- Rauwendaal C., Pol. Eng. Sci., vol 21, no. 16, p. 1092-100 (1981)
- Speur J.A., PhD.-thesis, University of Groningen, The Netherlands (1988)
- Todd D.B., Pol. Eng. Sci., vol. 15, no. 6, p. 437-43 (1975)

Appendix: The geometry of the extruder and its leakage flows

The extruder and its screws have the dimensions as indicated in the table below. The screws used are uniform, except in the feed zone in which among others the pitch is larger ($S = 30$ mm). In calculations, this effect is neglected, which is allowed since the extruder is only partially filled in that zone and not completely used.

Table 2.6 *Geometry of the screws*

Description	<i>symbol</i>	value
screw radius	R	$1.995 \cdot 10^{-2}$ m
pitch	S	$2.38 \cdot 10^{-2}$ m
number of thread starts	m	1
centre line distance	h_c	$3.50 \cdot 10^{-2}$ m
flight wall angle	ψ	0.122 rad
outer side width flight (y=H)	B_{fl}	$1.02 \cdot 10^{-2}$ m
chamber width (y=H)	W	$1.31 \cdot 10^{-2}$ m
chamber depth	H	0.0057 m
flight gap	δ	$5 \cdot 10^{-5}$ m
barrel width	b_s	$7.50 \cdot 10^{-2}$ m
screw length	L	0.600 m
calander gap	σ	$8.0 \cdot 10^{-4}$ m
side gap	ε	$1.0 \cdot 10^{-3}$ m
overlap angle	α_s	1.002 rad
number of chambers after injection point	V_{tot}	44

The counterrotating twin screw extruder

The leakage flows can be calculated by means of the equations given in this section. The leakage flows consist of non-pressure driven leakage flows and pressure driven leakage flows. The general form is:

$$Q_l = AN + B \frac{\Delta P_c}{\eta} \quad (2.7)$$

The geometrical constants can be calculated through:

$$A = 2(mA_s + mA_c + A_f) \quad (2.39)$$

and:

$$B = B_t + 2(mB_s + mB_c + B_f) \quad (2.40)$$

The various geometrical constants are given below.

Tetrahedron gap:

$$A_t = 0 \quad (2.41)$$

$$B_t = 0.0054R^3 \left(\frac{H}{R} \right)^{1.8} \left\{ \psi + 2 \left(\frac{\varepsilon + \sigma \tan \psi}{H} \right)^2 \right\} \quad (2.42)$$

with

$$\varepsilon = \frac{S}{2m} - B_{fl} - H * \tan \psi$$

Flight gap:

$$A_f = (2\pi - \alpha_s)R \left\{ \frac{S\delta}{2} + \frac{3S\delta^3(mS - B_{fl})}{6B_{fl}H^2} \right\} \quad (2.43)$$

$$B_f = (2\pi - \alpha_s)R \frac{\delta^3}{6B_{fl}} \quad (2.44)$$

Chapter 2

Calander gap:

$$A_c = \frac{4}{3} \pi \sigma (2R - H) \left(\frac{S}{m} - B_{fl} \right) \quad (2.45)$$

$$B_c = \frac{8m\sigma^2 \left(\frac{S}{m} - B_{fl} \right)}{9\pi \sqrt{(2R - H)}} \quad (2.46)$$

Side gap:

$$A_s = \pi (2R - H) (H - \sigma) (\varepsilon + \sigma \tan \psi) \quad (2.47)$$

$$B_s = \frac{m(H - \sigma) (\varepsilon + \sigma \tan \psi)^2 \cos^2 \psi}{12R \sin(\alpha/2)} * (1 - X) \quad (2.48)$$

with:

$$X = 0.630 \cos^2 \psi \left(\frac{\varepsilon + \sigma \tan \psi}{H - \sigma} \right) + 0.052 \left\{ \cos^2 \psi \left(\frac{\varepsilon + \sigma \tan \psi}{H - \sigma} \right) \right\}^5$$